Modeling the interplay between magnetic island dynamics and transport barrier formation

Julio J. Martinell[1], Stefany Cancino[1] and D. López-Bruna[2]

[1]*Instituto de Ciencias Nucleares, UNAM, A. Postal 70-543, México D.F., Mexico*

[2] *Laboratorio Nacional de Fusión, CIEMAT, 28040 Madrid, Spain*

I. Introduction. Some experiments [1] in stellarators have shown that the rational surfaces are the sites of an interesting relationship between MHD activity and transport barriers. Since magnetic islands usually form at rational surfaces it is hypothesized that the interplay between magnetic island dynamics and sheared flows around the islands takes place at these sites. The observed time evolution of bolometric signals from central and egde chords seen in Fig. 1 shows a periodic behavior with a sawtooth shape. The fast variation changes from a drop near the center to a rise near the edge and the inversion radius is at the rational surface. This is interpreted as a transport barrier at around the rational surface that is destroyed at the crash time. After this, a burst of MHD activity is detected in the $\dot{B}$ probes with frequency centered at 30 kHz and experiencing a down-shift. The likely process involved is that the MHD activity is due to an unstable tearing mode that makes an island at the resonant surface grow. Before, a transport barrier was formed around the rational surface and gets destroyed. The sequence of events that we want to explain is: (1) A small island rotating at high frequency is unstable and grows while reducing its rotation speed; (2) the resulting wide island gives rise to a sheared flow which in turn produces a transport barrier, (3) the transport barrier disappears leading also to a reduction or disappearance of the island.

II. Dynamics of magnetic islands The particular problem we have to address is that the vacuum island that is usually present at low-order rational surfaces is modified by the finite-beta, resistive plasma changing the width, w, and the relative phase, $\Delta\phi$. This can be considered in a way similar to the analysis of resonant magnetic perturbations (RMP). The study of tearing modes is separated in two regions: the MHD region, outside the resonant region and the non-ideal small inner region centered at the rational resonant surface. The two solutions are matched through the derivative jump parameter Δ'. The symmetric Δ'_c and antisymmetric Δ'_s parts of this parameter are related with the island growth and torque balance respectively. The first is written as the Rutherford equation

$$\frac{dw}{dt} = \frac{\rho_s^2}{\tau_R}(\Delta'_c + \Delta_{pol}) \quad \text{with,} \quad \Delta'_{pol} = \int \frac{dx}{\psi_0} \int \frac{d\alpha}{\pi} \int \frac{d\zeta}{2\pi} \frac{\sqrt{g}}{|\nabla\psi|} J_{pol} B \cos m\alpha.$$

while the net torques give the evolution of the phase difference $\Delta\phi$

$$\frac{d^2\Delta\phi}{dt^2} = N_V + N_{EM}, \tag{1}$$

where N_v is the viscous torque and the electromagnetic torque, is

$$N_{EM} = \int dx \int \frac{d\alpha}{\pi} \int \frac{d\zeta}{2\pi} \hat{\alpha} \cdot \mathbf{J} \times \mathbf{B} \frac{\sqrt{g}}{V'} = \frac{2\pi^2 \psi'}{\mu_0 b_t} m \psi_0^2 \Delta'_s$$

Here, $\alpha = \theta - m/n\zeta$ is the helical coordinate. The geometry is that of a helical stellarator. The island growth is determined by the two Δ terms. In presence of sheared flows the stability properties may change. In previous works it has been found that the presence of a sheared flow is stabilizing in the term Δ' [2]. There is however, a destabilizing region for intermediate shear values [3]. On the other hand, the second term is given by the presence of flows near the island separatrix produced by a polarization current. This effect has been evaluated for axisymmetric systems, having found to be stablizing for $\omega_{*i} < \omega < \omega_{*e}$ [4], but we need to compute it for non-axisymmetric geometry.

When there is torque imbalance, the phase shift change in (1), produces evolution of the rotation velocity, which would explain the observed frequency down-shift, until the torques balance. At this point, N_{EM} has a maximum and a minimum as function of rotation as seen in Fig. 2, while the viscous torque can be approximated by a straight line. Thus, there are multiple roots and reducing N_v can produce a bifurcation from a high ω to a low ω state. Once in the low branch, a second bifurcation can arise when N_v is increased, jumping then to a high rotation state [5]. The corresponding bifurcation process for the island width can be obtained as a function of the viscous torque, as shown in Fig. 3. As viscosity decreases for a small island, the bifurcation produces a large island width, while a subsequent increase of viscosity does not return through the same path but experiences a hysteresis; another threshold torque value is needed to get back to a small island.

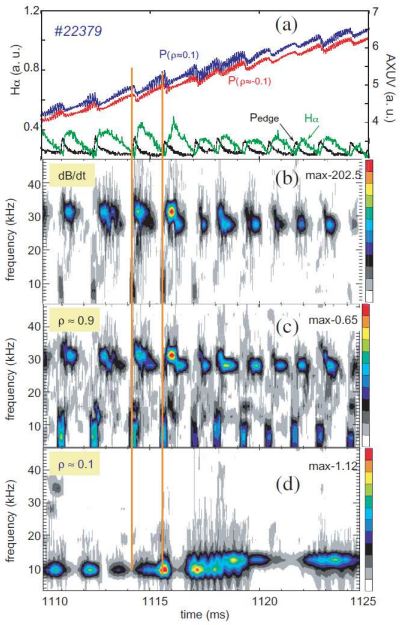

Figure 1: Experimental observations.

Regarding the viscous force, it turns out that it has an inverse dependence with the size of a boundary layer (BL) in the velocity profile that develops around the island [6]. This BL has the effect of shielding the island from external effects, allowing reconnection to occur. Now, since

most stellarators are in the $1/\nu$ collisionality regime, the viscosity grows as collisionality falls and, as a result, the BL decreases, thus hindering the reconnection. Inside the islands, the profiles may be flattened when the connection length along the filed lines is not too large, since in this case, the parallel transport relaxes the profiles across the island (flatness is $f = 0$). This happens for large islands, while a narrow island maintains cross gradients ($f = 1$). The island rotation velocity obtained from the frozen-in law and non-slip condition is [3] $\omega = f\omega_{*e} + (1-f)\omega_{*i}$.

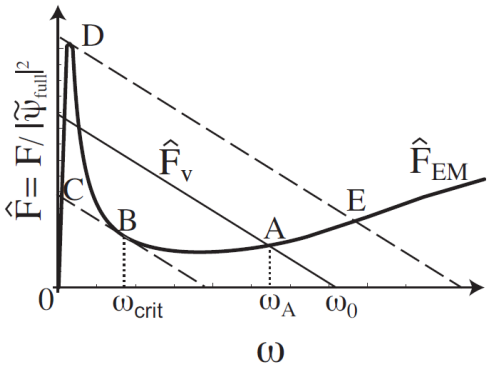

Figure 2: Torque balance showing tangent bifurcations.

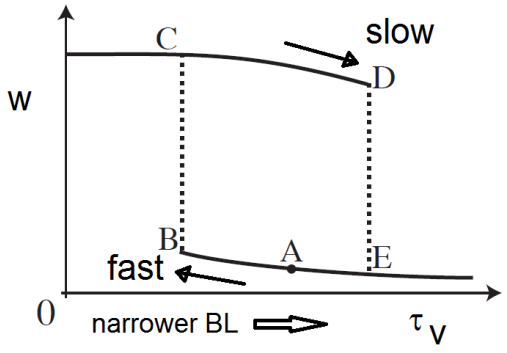

Figure 3: Island size dependence on viscous torque. Proposed cycle is shown.

III. Model for island-transport interplay. Based of all the facts mentioned above, we can envision the following sequence of events for explaining the observed evolution, based on the phenomenology of Fig. 3: (1) An initial (vacuum) magnetic island in presence of a finite-beta plasma experiences $E_r(r)$-field and rotates with $E \times B$ velocity ω_E [point A]. (2) Electron fluid around narrow island rotates at ω_{*e} in the frame where $E_r = 0$, since profiles inside narrow island are not flat, implying the electric field stays as in the outside (no shear flow). (3) Island grows by reconnection; viscous torque produces braking reaching $\omega = \omega_{*i}$. Phase shift evolves as there is torque unbalance; it settles at small $N_{EM} = N_v$ ($1/\nu$ regime). (4) At threshold torque, bifurcation arises [B to C], reaching critical width for profile flattening $w_m \sim \rho_s$ ($f = 0$ and no J_p effect) [equivalent to mode penetration of RMP]. (5) Across island, flat ϕ produces $E \sim 0$; the diamagnetic velocity jump across separatrix is balanced by E_r field. ω_E shear appears just outside separatrix, producing a transport barrier. BL layer around island is reduced and N_v grows to create a large island [like island healing [7]]. (6) Due to barrier, temperature rises locally reducing ν and increasing N_v; island width stays large until reverse bifurcation arises [D to E]; J_p then has a stabilizing effect: $\Delta_{pol} \leq 0$. The cycle thus repeats as temperature and N_v drop. The upper part of the cycle is slow, given by transport timescales, while the lower part is fast,

determined by the tearing mode processes that destabilize the island.

IV. Non-axisymmetric effect of Δ_{pol}. An important contribution to stability is the polarization current $J_p \sim J_\parallel - \langle J_\parallel \rangle$. We have computed the effect of non-axisymmetric geometry coming from the toroidal component of the $E \times B$ velocity. In stellarators $\vec{v}_E \cdot \nabla \psi$ includes toroidal variation which enters in J_p. The results obtained in [4] have an additional term,

$$J_p = [J_p]_C + \frac{\rho_s}{w} H' s \frac{\partial \phi}{\partial \alpha}$$

where $[J_p]_C$ is the result of [4]. We found that this will have a contribution to Δ_{pol} only for small ρ_s/w. Main contribution is from the separatrix where connection length s is largest. This can be shown to be destabilizing, $\Delta_{pol} > 0$. This is only relevant for low temperature, for small island widths. We can thus assure that J_p cannot be destabilizing for the range of interest $\omega \leq \omega_{*e}$.

V. Transport simulation model. This phenomenology is introduced in Astra transport code to simulate formation and disappearance of a transport barrier to try to reproduce observations in TJ-II. We take the shear flow of the form $\omega'_E = Kw$ according to the proposed behavior. The island width is made to vary as a fast growth (due to tearing mode reconnection) followed by slow reduction. An anomalous transport model based on resistive ballooning modes is used; the fluctuation level ε is determined by the growth rate and the shear flow stabilization, $\frac{\partial \varepsilon}{\partial t} = (\gamma_{RB} - \alpha_1 \varepsilon - \alpha_2 |\omega'_E|)\varepsilon - \nabla \cdot \Gamma_e$ This is added to neoclassical transport. Also, 3 carbon impurities are included in order to obtain the emission profiles. The resulting time evolution for different radii (chords) inside and outside the rational surface (located at $\rho = .75$) is shown in Fig. 4. As it can be observed, it reproduces the observations, including the crash inversion radius. We still have to self-consistently include the island evolution in the modeling.

Acknowledgements. This work was partially supported by projects DGAPA-UNAM IN109115 and CONACyT 152905.

References

[1] D. López-Bruna el al., Nuclear Fusion **53**, 073051 (2013).

[2] P.A. Cassak, Phys. Plasmas **18**, 072106 (2011).

[3] R. Fitzpatrick and F.L. Waelbroeck, Phys. Plasmas **16**, 052502 (2009).

[4] J.W. Connor, F.L. Waelbroeck and H.R. Wilson, Phys. Plasmas **8**, 2835 (2001).

[5] F.L. Waelbroeck, Nucl. Fusion **49**, 104025 (2009).

[6] C.C. Hegna, Nucl. Fusion, **51**, 113017, (2011).

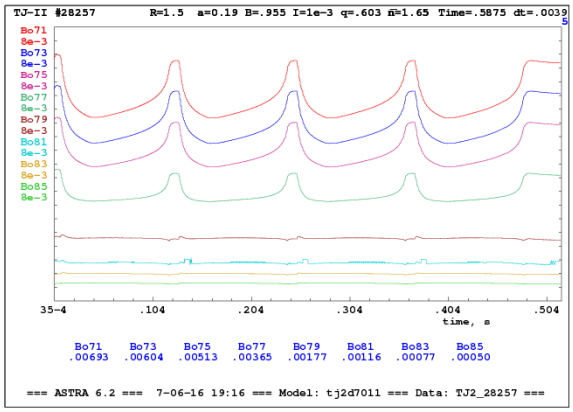

Figure 4: Bolometer emission time evolution.